Available online at www.sciencedirect.com
ScienceDirect
Journal of Photochemistry and Photobiology A: Chemistry 184 (2006) 193–203
Journal of Photochemistry and Photobiology A:Chemistry
www.elsevier.com/locate/jphotochem

Spectroscopic and electrochemical properties of new amphiphilic donor–acceptor conjugated polyenes

Beata W. Domagalska [a,*], Kazimiera A. Wilk [a], Ryszard Zieliński [b]

[a] *Faculty of Chemistry, Wrocław University of Technology, ul. Wybrzeże Wyspiańskiego 27, 50-370 Wroclaw, Poland*
[b] *Department of Technology and Environmental Protection, Poznań University of Economics, Al. Niepodległości 10, 60-967 Poznań, Poland*

Received 15 February 2006; received in revised form 10 April 2006; accepted 12 April 2006
Available online 28 April 2006

Abstract

New, terminally substituted, unsymmetrical conjugated polyenes $ROC_6H_4(CH{=}CH)_nTB$ (TB = l,3-diethyl-thioxodihydropyrimidine-4,6-dione: R = CH_3 (n = 4, 6); R = C_6H_{13} (n = l, 2, 3, 4, 5, 6)) $ROC_6H_4(CH{=}CH)_nID$ (ID = indan-l,3-dione: R = CH_3, C_6H_{13} (n = 4, 6)), and $ROC_6H_4(CH{=}CH)_nPN$ (PN = phenylacetonitrile R = CH_3, C_6H_{13} (n = 4, 6)) were synthesized through Knoevenagel condensation of respective ω-(*p*-alkyloxyphenyl)polyenals and benzyl cyanide (A = PN), indandione (A = ID) and *N*,*N*′-diethylthiobarbituric acid (A = TB). These compounds show a remarkable thermal stability with decomposition temperatures ranging from 133 to 291 °C. For all obtained *push-pull* polyenes, the shift of λ_{max} to longer wavelength was observed as a function of the increasing conjugated system size as well as the donor–acceptor (D–A) pair strength. The inverted solvatochromic effect appeared with the increase of solvent polarity. The redox properties of the studied compounds were investigated applying the cyclic voltammetry technique (CV). Electrochemically evaluated band gap values are well correlated with the optical data.

Keywords: *Push-pull* conjugated polyenes; Thermal stability; Redox properties; Solvatochromic effect

1. Introduction

Long π-conjugated polyenic structures grafted by an electron donor (D) and an electron acceptor (A) group (*push-pull* polyenes) have recently been a subject of broad experimental and theoretical investigations [1–10]. *Push-pull* polyenes, in most cases, exhibit large ground-state dipole moments, allowed low lying electronic transitions, substantial changes in dipole moment upon the excitation [11], solvent polarity effects on steady-state fluorescence spectra, and fluorescence intensity decay, formation of excited-state charge-transfer (CT) state [12,13], as well as aggregation phenomena at interfaces [14]. Their physicochemical behavior makes them convenient model molecules for both theoretical analysis of the electroactive groups influence upon the geometric and electronic polyenic structures, and their forecasting properties. Studies on fundamental photochemical processes in naturally occurred polyenes and carotenoids have already introduced many profound achievements in the area of: various kinetic models (e.g., three-state kinetic model [15]), solvatokinetic behavior [16], nature of excited states [17], influence description of donor and acceptor groups on kinetics of the competitive (radiative, reactive, and non-radiative) relaxation pathways and the photoreaction mechanism [17], light harvesting responses [18,19], redox switching phenomena [20], and defensive pheromone mechanisms [21]. The D-π-A systems have also revealed high non-linear optical properties [11], which are an important prerequisite for potential application in data storage, holographic materials, optical switches, or molecular wires [22].

The present work is a continuation of our search for new D-π-A compounds with potential photo or/and electroconducting properties [7–10,23,24], especially designated for a solar cell. Previously, we have designed the modular synthesis of stereo defined (pure *all-E*) long π-conjugated polyenals of both unsymmetrical, symmetrical (two-dimensional), and octupolar-type structures [7,8] which are convenient reagents for synthese of *push-pull*, *push-push*, and *pull-pull* polyenes [3]. The reported ω-(*p*-alkyloxyphenyl)polyenals with up to 10 conjugated double

* Corresponding author. Tel.: +48 71 3203849; fax: +48 71 3203678.
E-mail address: beata.domagalska@pwr.wroc.pl (B.W. Domagalska).

1010-6030/$ – see front matter © 2006 Elsevier B.V. All rights reserved.
doi:10.1016/j.jphotochem.2006.04.015

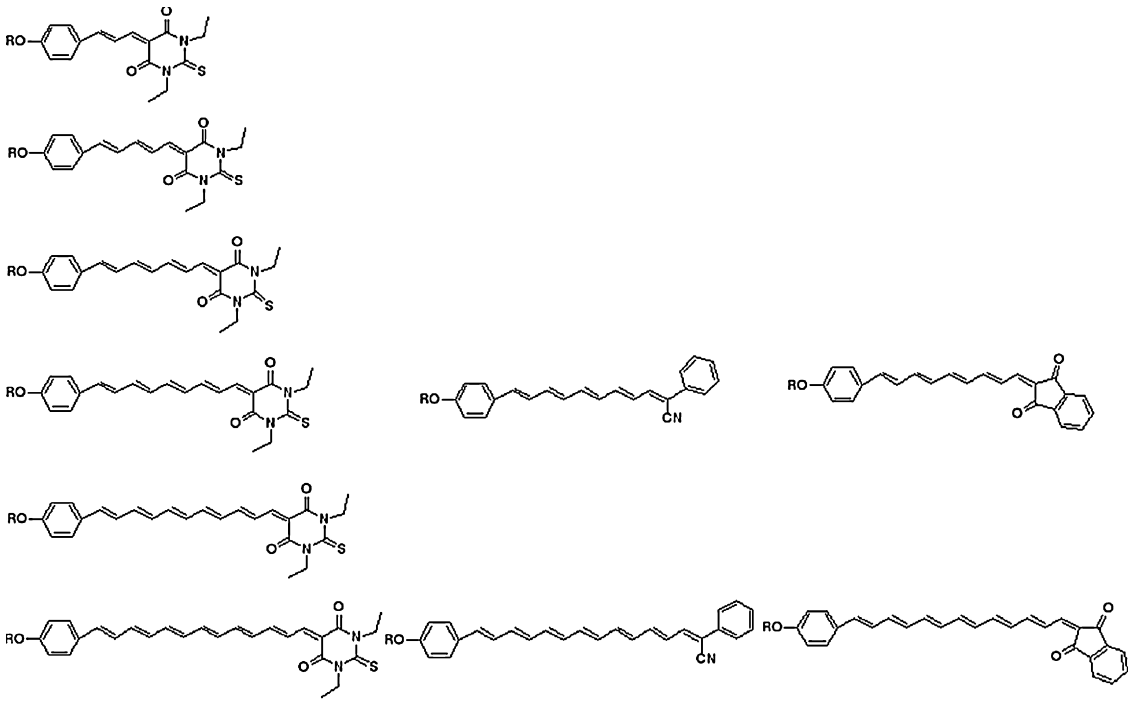

R	n	n_{eff}[a)]	Abbreviation
CH_3	4, 6	7, 9	$ROC_6H_4(CH{=}CH)_nTB$
n-C_6H_{13}	1, 2, 3, 4, 5, 6	4, 5, 6, 7, 8, 9	
CH_3	4, 6	9, 11	$ROC_6H_4(CH{=}CH)_nPN$
n-C_6H_{13}	4, 6	9, 11	
CH_3	4, 6	7, 9	$ROC_6H_4(CH{=}CH)_nID$
n-C_6H_{13}	4, 6	7, 9	

a) $ROC_6H_4(CH{=}CH)_nTB$: n_{eff}= n+2+1, $ROC_6H_4(CH{=}CH)_nCP$: n_{eff}= n+2+3; $ROC_6H_4(CH{=}CH)_nID$: n_{eff}= n+2+1

Fig. 1. Molecular structure of studied conjugated *push-pull* polyenes.

bonds, posses interesting NLO properties [9]. Furthermore, the increase of their solvent polarity causes the shift of the canonical polyenal structure from a more polymethine-like to more polyene-like state [10]. Polyenal molecules were found to lay flat on the water subphase with their hydrophobic tail elevated and such monolayers are ohmic conductors which conductivity depends on NO_2 concentration and is relatively high at room temperature [24]. The main purpose of the present contribution was to graft the alkoxylphenyl polyenal backbone by 1,3-diethyl-thioxodihydropyrimidine-4,6-dione (TB), indan-l,3-dione (ID), and phenylacetonitrile (PN) grouping (for the compounds' structures and abbreviations see Fig. 1) in order to get new thermally stable products and to characterize their spectroscopic and electrochemical behavior in a variety of solvents. Thus, we have concentrated our attempts on investigating any available changes in shape and position of the absorption band in relation to both the polyenic linker, and alkyl chain length, as well as the kind of solvent and the A (A = TB, ID, and PN) group π-accepting effect. Additionally, we examined the reduction and oxidation potentials for all studied D-π-A compounds, especially the relative strength of the A acceptor and the effect of the effective conjugation length -"n_{eff}" on the values of the oxydation (E_{ox}) and reduction (E_{red}) potentials as well as on the total number of their redox states. The reported compounds exhibit a typical semiconducting behavior and for derivatives with ID grouping the electrical conductivity increases more than two orders of magnitude under the white light exposure (intensity about 10 mW cm^{-2}) and such investigations are in progress [25].

2. Experimental

2.1. General methods

Syntheses involving polyenes were carried out under argon, with the protection against direct daylight. The chromatographic purification was accomplished by the medium pressure

column chromatography (MPLC, Büchi Labortechnik AG, silica gel, flow rate 20 ml min^{-1}, eluent–hexane: ethyl acetate 3:1) and/or radial chromatography (Chromatotron, Harrison Research Inc., N_2, 2 mm layer of silica gel, flow rate 6 ml min^{-1}, eluent–hexane: ethyl acetate 4:1). The thermal stability of synthesized compounds was determined with the Shimadzu's thermogravimetrical analyzer (TGA-50), differential thermal analyzer (DTA-50) and the differential scanning calorimeter (DSC-50). Samples were analyzed in alumina crucibles using α-Al_2O_3 as a reference substance over the temperature ranging from 20 °C to 450 °C. In all analyzers the heating rate was 10 °C/min and the sampling frequency of 0.5 s was applied. Nuclear magnetic resonance (NMR) spectra were recorded with a Bruker AMX-300 spectrometer (Karlsruhe, Germany). ^{1}H chemical shifts (at 300.13 MHz) are referenced in $CDCl_3$ to residual protons of $CHCl_3$ (7.24 ppm). Elemental analyzes were carried out with a Perkin-Elmer 2400 CHN analyzer (Norwalk, CT). Solvents (2,2,4-trimethylpentane, carbon tetrachloride, tetrahydrofuran, dichlorometane, ethanol, methanol, and acetonitrile) were spectroscopic grade (Merck or Sigma–Aldrich). The UV–vis absorption spectra of freshly prepared solutions of studied polyenals (concentration 5×10^{-6} M) were measured at room temperature using UV–vis Unicam (thermo Spectronic) spectrophotometer. Spectra were recorded in teflon–stopped quartz cells of 1 cm optical pathlength within the range from 205 to 600 nm for 2,2,4-trimethylpentane, ethanol, methanol, and acetonitrile solutions and from 250 to 600 nm for carbon tetrachloride, tetrahydrofuran, dichlorometane solutions. The CV experiments were carried out using the standard three-electrode system with a platinium plate as an auxiliary electrode and the working platinium electrode by means of Universal Electrochemical Set (EMU, Wroclaw University of Technology, Poland). The cyclic voltammograms were recorded at 100–1000 mV/s for $ROC_6H_4(CH{=}CH)_nID$ and $ROC_6H_4(CH{=}CH)_nTB$ and in the range 50–1000 mV/s for $ROC_6H_4(CH{=}CH)_nPN$, with a platinium working electrode (2.01 mm^2) and a saturated calomel electrode (SCE) or Ag/AgCl as the reference electrode using tetrabutylammonium tetrafluroborate ($TBABF_4$, reduction) or tetrabutylammonium hexafluorophosphate ($TBAPF_6$, oxidation) as supporting electrolytes. Electrochemical cell was protected against light during CV measurements. All samples were deoxidized by bubbling the oxygen-free nitrogen ($O_2 < 5$ ppm, LINDE Gaz) and a special grade argon before measurements.

2.2. Synthesis of conjugatedpolyenes $ROC_6H_4(CH{=}CH)_nA$ (A = TB, ID)

The appropriate alkoxyphenylpolyenal was dissolved in warm anhydrous ethanol (20 ml/mmol) and then added to warm solution of indandione or *N*,*N*′-diethylthobarbituric acid (1.1 equivalent) in hot ethanol. The mixture was heated under reflux. If a color change did not occur swiftly, catalytic KOH (one drop of 0.3% EtOH solution) was added and the reaction continued until TLC indicated that the reaction was complete (0.5–6 h). Unless the product preferentially crystallized, the ethanol was evaporated and residue eluted by chromatographic method.

$C_6H_{13}OC_6H_4(CH{=}CH)_1TB$. Yellow needle. Yield 92%. Anal. calc. for $C_{23}H_{30}N_2O_3S$ (414.56): C 65.64, H 7.51 N 6.96, S 7.96; found C 65.39, H 7.80 N 7.12, S 7.80; ^{1}H NMR: 8.50 (1H, dd, *J* = 12.1, 15.3 Hz), 8.15 (1H, d, *J* = 12.1 Hz), 7.43 (1H, d, *J* = 15.0 Hz), 7.1 (2H, d, *J* = 8.8 Hz), 6.8 (2H, d, *J* = 8.9 Hz), 4.57 (4H, q, *J* = 6.8 Hz) 3.99 (2H, t, *J* = 6.6 Hz), 1.81 (2H, m), 1.47–1.28 (10H, m) 1.46 (2H, m), 0.90 (3H, t, *J* = 6.9 Hz).

$C_6H_{13}OC_6H_4(CH{=}CH)_2TB$. Red powder. Yield 88%. Anal. calc. for $C_{25}H_{32}N_2O_3S$ (440.60): C 67.26, H 7.53 N 6.54, S 7.48; found C 67.35, H 7.39 N 6.61, S 7.35; ^{1}H NMR: 8.15 (1H, d, *J* = 12.7 Hz), 8.05 (1H, t, *J* = 13.0 Hz), 7.41 (2H, d, *J* = 9,3 Hz), 6.62 (2H, d, *J* = 9,3 Hz), 7.33 (1H, dd, *J* = 13.4, 11.0 Hz), 7.06 (1H, d, *J* = 14.65 Hz), 6.93 (1H, dd, *J* = 14,9, 11,0 Hz), 4.57 (4H, q, *J* = 7.0 Hz) 3.99 (2H, t, *J* = 6.6 Hz), 1.81 (2H, m), 1.46–1.28 (10H, m) 1.46 (2H, m), 0.90 (3H, t, *J* = 6.9 Hz).

$C_6H_{13}OC_6H_4(CH{=}CH)_3TB$. Dark violet solid. Yield 88%. Anal. calc. for $C_{27}H_{34}N_2O_3S$ (466.63): C 68.69, H 7.54 N 6.15, S 7.05; found C 68.48, H 7.81 N 6.16, S 7.20; ^{1}H NMR: 8.09 (1H, d, *J* = 12.8 Hz), 7.99 (1H, t, *J* = 13.4 Hz), 7.1–6.98 (3H, m), 7.25 (1H, dd, *J* = 13.4, 11.8 Hz), 6.96 (1H, dd, *J* = 14.2, 10.4 Hz), 6.87 (1H, d, *J* = 15.0 Hz), 6.76–6.82 (3H, m), 6.57 (1H, dd, *J* = 13.9, 12.3 Hz), 4.57 (4H, q, *J* = 6.8 Hz) 3.99 (2H, t, *J* = 6.6 Hz), 1.81 (2H, m), 1.46–1.28 (10H, m) 1.45 (2H, m), 0.91 (3H,t, *J* = 6.9 Hz).

$CH_3OC_6H_4(CH{=}CH)_4TB$. Dark violet solid. Yield 75%. Anal. calc. for $C_{24}H_{26}N_2O_3S$ (422.54): C 67.29, H 6.38 N 6.82, S 7.81; found C 67.11, H 6.56 N 6.69, S 7.92; ^{1}H NMR: 8.08 (1H, d, *J* = 12.7 Hz), 7.99 (1H, dd, *J* = 13.5, 12.8 Hz), 7.41 (2H, d, *J* = 8.9 Hz), 7.22 (1H, dd, *J* = 13.5, 12.0 Hz), 6.69 (2H, d, *J* = 8.9 Hz), 6.88 (1H, dd, *J* = 14.2, 11.6 Hz), 6.72 (4H, m), 6.55 (1H, dd, *J* = 14.3, 11.9 Hz), 4.56 (4H, q, *J* = 6.9 Hz), 3.78 (3H, s), 1.20 (6H, 2t, *J* = 7.0 Hz).

$C_6H_{13}OC_6H_4(CH{=}CH)_4TB$. Dark violet solid. Yield 72%. Anal. calc. for $C_{29}H_{36}N_2O_3S$ (492.67): C 70.70, H 7.37 N 5.69, S 6.51; found C 70.12, H 7.79 N 5.66, S 6.77; ^{1}H NMR: 8.08 (1H, d, *J* = 12.7 Hz), 7.99 (1H, dd, *J* = 13.5, 12.8 Hz), 7.41 (2H, d, *J* = 8.9 Hz), 7.22 (1H, dd, *J* = 13.5, *J* = 12.0 Hz), 6.69 (2H, d, *J* = 8.9 Hz), 6.88 (1H, dd, *J* = 14.2, *J* = 11.6 Hz), 6.72 (4H, m), 6.55 (1H, dd, *J* = 14.3, 11.9 Hz), 4.57 (4H, q, *J* = 6.8 Hz) 3.99 (2H, t, *J* = 6.6 Hz), 1.81 (2H, m), 1.46–1.28 (10H, m) 1.46 (2H, m), 0.90 (3H, t, *J* = 6.9 Hz).

$C_6H_{13}OC_6H_4(CH{=}CH)_5TB$. Brown solid. Yield 68%. Anal. calc. for $C_{31}H_{38}N_2O_3S$ (518.71): C 71.11, H 7.56 N 5.53, S 6.32; found C 71.00, H 7.68 N 5.23, S 6.45; ^{1}H NMR: 8.10 (1H, d, *J* = 12.7 Hz), 8.02 (1H, dd, *J* = 13.8, 12.1 Hz), 7.33 (2H, d, *J* = 8.8 Hz), 7.22 (1H, dd, *J* = 13.6, 12.0 Hz), 6.69 (2H, d, *J* = 8.8 Hz), 6.88–6.69 (7H, m), 6.55 (1H, dd, *J* = 14.3, 11.9 Hz), 4.57 (4H, q, *J* = 6.8 Hz) 3.99 (2H,t, *J* = 6.6 Hz), 1.81 (2H, m), 1.47–1.26 (10H, m) 1.46 (2H, m), 0.90 (3H, t, *J* = 6.9 Hz).

$CH_3OC_6H_4(CH{=}CH)_6TB$. Dark brown solid. Yield 67%. Anal. calc. for $C_{28}H_{30}N_2O_3S$ (474.61): C 70.86, H 6.38 N 5.91, S 6.74; found C 70.64, H 6.55 N 6.03, S 6,50; ^{1}H NMR: 8.10 (1H, d, *J* = 12.1 Hz), 7.99 (1H, dd, *J* = 13.5, 12.5 Hz), 7.31 (2H, d, *J* = 8.9 Hz), 7.26 (1H, dd, *J* = 13.5, 12.0), 6.88 (1H, dd, *J* = 14.2, 11.6 Hz), 6.79–6.65 (10H, m), 6.58 (1H, dd, *J* = 14.3,

11.9 Hz), 4.56 (4H, q, J = 6.9 Hz), 3.78 (3H, s), 1.20 (6H, 2t, J = 7.0 Hz).

C6H13OC6H4(CH=CH)6TB. Dark brown solid. Yield 65%. Anal. calc. for $C_{33}H_{40}N_2O_3S$ (544.75): C 65.39, H 7.57 N 5.26, S 6.01; found C 65.18, H 7.88 N 5.05, S 5.92; ^{1}H NMR: 8.05 (1H, d, J = 12.1 Hz), 7.97 (1H, dd, J = 13.5, 12.5 Hz), 7.30 (2H, d, J = 8.9 Hz), 7.25 (1H, dd, J = 13.5, 12.0 Hz), 6.89 (1H, dd, J = 14.2, 11.6 Hz), 6.79–6.66 (10H, m), 6.57 (1H, dd, J = 14.3, 11.9 Hz), 4.57 (4H, q, J = 6.8 Hz), 3.99 (2H, t, J = 6.6 Hz), 1.81 (2H, m), 1.46–1.28 (10H, m), 1.46 (2H, m), 0.90 (3H,t, J = 6.9 Hz).

CH3OC6H4(CH=CH)4ID. Brown solid. Yield 68%. Anal. calc. for $C_{25}H_{20}O_3$ (368.44): C 81.50, H 5.47; found C 81.40, H 5.66. ^{1}H NMR: 8.14 (1H, d, J = 12.4 Hz), 7.93–7,99 (3H, m), 7.78 (2H, m), 7.31 (2H, d, J = 8.9 Hz), 7.22 (1H, dd, J = 14.3, 12.1 Hz), 6.85 (1H, dd, J = 14.8, 11.0 Hz), 6.72–7.80 (5H, m), 6.58 (1H, dd, J = 14.4, 11.0 Hz), 6.77 (1H, d, J = 14.5 Hz), 3,78 (3H, s).

C6H13OC6H4(CH=CH)4ID. Brown solid. Yield 60%. Anal. calc. for $C_{30}H_{30}O_3$ (438,57): C 82.16, H 6.89; found C 81.60, H 7.01. ^{1}H NMR: 8.12 (1H, d, J = 12.5 Hz), 7.90–7.97 (3H, m), 7.78 (2H, m), 7.31 (2H, d, J = 8.9 Hz), 7.22 (1H, dd, J = 14.3, 12.1 Hz), 6.85 (1H, dd, J = 14.9, 11.1 Hz), 6.74–7.79 (5H, m), 6.55 (1H, dd, J = 14.6, 11.0 Hz), 6.75 (1H, d, J = 14.7 Hz), 4.0 (2H, t, J = 6.8 Hz), 1.81 (2H, m), 1.46–1.28 (6H, m), 0.91 (3H, t, J = 7.0 Hz).

CH3OC6H4(CH=CH)6ID. Dark brown solid. Yield 59%. Anal. calc. for $C_{29}H_{24}O_3$ (420.50): C 82.82, H 5.76; found C 82.61, H 5.97 ^{1}H NMR: 8.12 (1H, d, J = 12.0 Hz), 7.93–7.99 (3H, m), 7.78 (2H, m), 7.31 (2H, d, J = 8.9 Hz), 7.25 (1H, dd, J = 13.6, 12.0 Hz), 6.87 (1H, dd, J = 14.3, 11.3 Hz), 6.79–7.22 (9H, m,), 6.58 (1H, dd, J = 14.4, 11.1 Hz), 6.77 (1H, d, J = 14,4 Hz), 3.78 (3H, s).

C6H13OC6H4(CH=CH)6ID. Dark brown solid. Yield 59%. Anal. calc. for $C_{34}H_{34}O_3$ (490.64): C 81.55, H 8.86; found C 81.28, H 8.99 ^{1}H NMR: 8.12 (1H, d, J = 12.0 Hz), 7.93–7.96 (3H, m), 7.80 (2H, m), 7.30 (2H, d, J = 8.9 Hz), 7.24 (1H, dd, J = 13.6, 12.0 Hz), 6.87 (1H, dd, J = 14.3, 11.3 Hz), 6.79–7.22 (9H, m), 6.58 (1H, dd, J = 14.4, 11.1 Hz), 6.77 (1H, d, J = 14,4 Hz), 3.99 (2H, t, J = 6.6 Hz), 1.81 (2H, m), 1.46–1.28 (6H, m), 0.90 (3H, t, J = 6.9 Hz).

2.3. Synthesis of conjugated polyenes ROC6H4(CH=CH)nPN

A solution of corresponding polyenal (0.5 mmol), benzyl cyanide (1 mmol), ammonium acetate (25 mg, 0.23 mmol), and acetic acid (1 ml) in toluene (30 ml) was refluxed with azeotropic distillation using a Dean-Stark for 24 h. The solvent was removed under reduced pressure and the isolation of the final products was performed by careful flash chromatography.

CH3OC6H4(CH=CH)4PN. Dark orange solid. Yield 68%); Anal. calc. for $C_{24}H_{21}NO$ (339.43): C 84.92, H 6.24, N 4,13; found C 84.66, H 6.24, N 4.00 ^{1}H NMR: 7.61 (2H, d, J = 8.8 Hz), 7.38–7.45 (6H, m), 6.89 (2H, d, J = 8.9 Hz), 6.88–6.47 (8H, m), 4.0 (3H, s).

C6H13OC6H4(CH=CH)4PN. Dark orange solid. Yield 62%; Anal. calc. for $C_{29}H_{31}NO$ (409.57): C 85.04, H 7.63, N 3.42; found C 84.90, H 7.90, N 3.18 ^{1}H NMR: 7.61 (2H, d, J = 8.8 Hz), 7.38–7.45(6H, m), 6.89 (2H, d, J = 8.9 Hz), 6.88–6.47 (8H, m), 4.0 (2H, t, J = 6.6 Hz), 1.81 (2H, m), 1,47 (2H, m), 1.46–1.28 (4H, m), 0.90 (3H, t, J = 6.9 Hz).

CH3OC6H4(CH=CH)6PN. Dark orange solid. Yield 58%; Anal. calc. for $C_{28}H_{25}NO$ (391.51): C 73.81, H 6.20, N 3.59; found C 73.78, H 6.29, N 3.52 ^{1}H NMR: 7.63 (2H, d, J = 8.7), 7.38–7.45 (8H, m), 6.90 (2H, d, J = 8.9 Hz), 6.87–6.45 (10H, m), 3.95 (3H, s).

C6H13OC6H4(CH=CH)6PN. Dark orange solid. Yield 54%; Anal. calc. for $C_{33}H_{35}NO$ (461.64): C 85.90 H 6.44, N 3.58; found C 85.85, H 6.38, N 3.49 ^{1}H NMR: 7.60 (2H, d, J = 9.0 Hz), 7.35–7.47 (8H, m), 6.87 (2H, d, J = 8.9 Hz), 6.85–6.43 (10H, m), 4.0 (2H, t, J = 6.6 Hz), 1.79 (2H, m), 1.46 (2H, m), 1.46–1.25 (4H, m), 0.91 (3H, t, J = 6.9 Hz).

3. Results and discussion

The studied polyenic derivatives $CH_3OC_6H_4(CH{=}CH)_nA$ (n = 4, 6 for A = 1,3-diethyl-thioxodihydropyrimidine-4,6-dione (TB), indan-l,3-dione (ID) and phenylacetonitrile (PN)) and $C_6H_{13}OC_6H_4(CH{=}CH)_nA$ (n = 1, 2, 3, 4, 5, 6 for A = TB and n = 4, 6 for A = ID and PN) were synthesized by the condensation reaction of respective ω-(*p*-alkyloxyphenyl)polyenals [7] with benzyl cyanide, 1,3-indandione or *N*,*N*′-diethylthiobarbituric acid according to the literature directions [26,27]. The presence of both hydrophobic moieties (*n*-hexyloxy chain and long conjugated system) and of the hydrophilic acceptor entity confers an amphiphilic character of these D-π-A derivatives. The molecular structures of all newly synthesized *push-pull* polyenes were confirmed by the elemental analysis, by one- and two-dimensional NMR, as well as by UV–vis spectra. The ^{1}H NMR spectra of $ROC_6H_4(CH{=}CH)_nA$ indicate two groups of signals: the first group – at the range of δ = 5.0–0.8 ppm due to aliphatic chain protons, and the second group – at the range of δ = 9.5–5.0 ppm due to aromatic and olefinic protons. In the case of spectra of thiobarbituric acid derivatives one can additionally observe a multiplet at about 4.5 ppm and a triplet at about 1.25 ($J \approx 7$ Hz). These signals are unambiguously related to protons of the *N*-CH_2 and *N*-CH_2CH_3 groups, respectively. Moreover, for the benzyl cyanide-derived compounds an additional multiplet in the aromatic part of spectra ($\delta \approx 7.3$ ppm) can be assigned to protons of monosubstituted phenyl ring. For the 1,3-indandione-based representative two multiplets at 7.9 and 7.8 ppm can be attributed to four protons of the indandione moiety (AABB spin system) [28].

According to the cited reference [29], the amount of information obtainable from single resonance spectra for compounds of more than four double bonds in the conjugated backbone is limited mainly due to complexity and extensive overlapping the resonance signals. Thus, the structure and stereochemistry of $ROC_6H_4(CH{=}CH)_nA$ containing more than four conjugated double bonds have been studied by ^{1}H NMR spectroscopy using one- (^{1}H) and two-dimensional spectra (^{1}H-^{1}H correlated spectroscopy—COSY). At 300 MHz these

Table 1
Thermal characteristics of $ROC_6H_4(CH{=}CH)_nA$

R	n	n_{eff}	T_m[a] (°C)	ΔH_m (kJ/mol)	T_{do}[b] (°C)	T_{dm}[c] (°C)
$ROC_6H_4(CH{=}CH)_nTB$						
CH_3	4	7	152[d]	–	152[d]	275
	6	9	133[d]	–	133[d]	290
C_6H_{13}	1	4	147.1	45.6	233	291
	2	5	131.7	40.7	210	245
	3	6	148.8	35.7	158	273
	4	7	150[d]	–	150[d]	267
	5	8	135[d]	–	135[d]	276
	6	9	136[d]	–	136[d]	289
$ROC_6H_4(CH{=}CH)_nPN$						
CH_3	4	9	154.5	27.9	187	265
	6	11	158[d]	–	158[d]	283
C_6H_{13}	4	9	127	28,3	170	251
	6	11	160[d]	–	160[d]	271
$ROC_6H_4(CH{=}CH)_nID$						
CH_3	4	7	149	28.4	190	278
	6	9	289[d]	–	289[d]	350
C_6H_{13}	4	7	137	32.2	195	290
	6	9	291[d]		289[d]	360

[a] Melting point.
[b] Onset of decomposition.
[c] Maximum of the decomposition exotherm.
[d] Melting with partial decomposition.

two methods provided the necessary identification of almost all protons of studied polyenic chains and determination of coupling constants; the vicinal ones across the double bonds are ca. 15, 12, and 14.5 Hz for compounds with A = PN, ID and TB, respectively. The values of ^3J coupling constants (across single carbon–carbon bonds) are within the range of 11–12 Hz. Thus, accordingly to the above mentioned methods it can be concluded that the conjugated system is in the *all*-E configuration and the polyenic chain (as in reference [29]) constitutes a nearly planar arrangement. Moreover, the introduction of new acceptor groups by means of the Knoevenagel condensation does not lead to the configuration change of the polyenic backbone. Recalling [26], the difference in the value of $^3J_{HH}$ coupling constants (ΔJ) for CH=CH and CH–CH enables one to estimate the canonical charge-transfer resonance structure of conjugated polyenes. For $ROC_6H_4(CH{=}CH)_nPN$, $ROC_6H_4(CH{=}CH)_6ID$, and $ROC_6H_4(CH{=}CH)_nTB$ the ΔJ values were calculated as 4.5, 2.4, 2.5 Hz, respectively, indicating that the contribution of the zwitterionic form to the ground state of indandione and thiobarbituric acid derivatives in $CDCl_3$ solution is higher in relation to benzyl cyanide derivatives or polyenals (ΔJ = 2.5 Hz [10]).

3.1. Thermal stability

Thermal stability of chromophores along with high nonlinearity and photostability are essential for potential applications in electrooptical modulators. Practically useful materials should be chemically and physically stable at continuous operating temperatures of 80 °C and at intermittent device processing temperatures above 250 °C [30,31].

We investigated the thermal stability of all *push-pull* polyenes $ROC_6H_4(CH{=}CH)_nA$ by means of the following methods: differential scanning calorimetry, thermogravimetry, and differential thermal analysis. These measurements provide a complex thermal characteristics of the studied polyenes and in Table 1 there are collected the following stability parameters: the values of T_m (melting point), as well as T_{do} (onset of decomposition), T_{dm} (maximum of the decomposition exotherm). Typical DSC and TGA curves for $C_6H_{13}OC_6H_4(CH{=}CH)_3TB$ are depicted in Fig. 2.

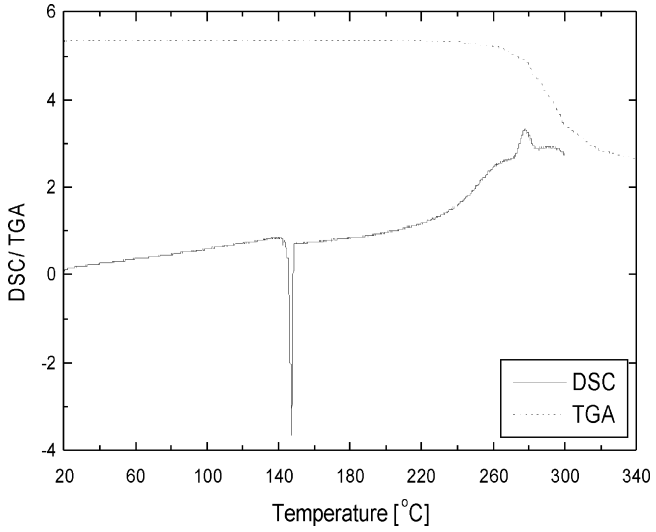

Fig. 2. DSC and TGA plots for $C_6H_{13}OC_6H_4(CH{=}CH)_3TB$.

Table 2
Experimental solvent effects on the first π–π^* transition of studied $ROC_6H_4(CH{=}CH)_nA$

R	n	n_{eff}	TMP	CCl_4	THF	CH_2Cl_2	C_2H_5OH	CH_3OH	CH_3CN
$ROC_6H_4(CH{=}CH)_nTB$									
CH_3	4	7	535	533	532	541	550	542	526
	6	9	592	588	587	605	608	601	587
C_6H_{13}	1	4	433	431	430	437	445	436	425
	2	5	461	466	459	467	483	475	453
	3	6	490	504	507	516	519	509	502
	4	7	533	531	529	544	550	541	529
	5	8	568	559	566	575	582	572	558
	6	9	593	586	588	603	607	600	586
$ROC_6H_4(CH{=}CH)_nPN$									
CH_3	4	9	428	428	433	431	431	426	426
	6	11	445	447	450	449	447	440	443
C_6H_{13}	4	9	441	441	447	446	446	442	444
	6	11	446	445	449	448	448	441	445
$ROC_6H_4(CH{=}CH)_nID$									
CH_3	4	7	457	458	462	457	465	465	466
	6	9	478	489	488	499	493	490	485
C_6H_{13}	4	7	455	461	463	474	467	464	465
	6	9	475	487	489	498	493	491	484

Push-pull polyenes containing 4 double bonds for A = PN and ID and 1, 2, and 3 double bonds for A = TB exhibits a clear single signal in the DSC curve due to the sample melting. It is interesting to note that we have not observed any solid–solid transitions at temperatures below the sample melting. A thorough analysis of the DTA curves allows one to conclude that all samples are thermally stable up to at least 133 °C. The data collected in Table 1 reveal, in general, that

Table 3
Redox potentials (E_{ox}, E_{red}) and calculated optical (E_g^{op}) and electrochemical (E_g^{cv}) band gap of synthesized amphiphilic conjugated polyenes $ROC_6H_4(CH{=}CH)_nA$ at 25 °C

R	n	n_{eff}	λ_{onset} [a]	E_g^{opt} [b] (eV)	E_{ox} [c] Pt vs. SCE (V)	E_{ox} [d] Pt vs. Ag/AgCl (V)	E_{red}^{calc} [e] (V)	E_{red} [c] Pt vs. SCE (V)	E_g^{CV} [f] (V)
$ROC_6H_4(CH{=}CH)_nTB$									
CH_3	4	7	639	1.94	1.09	0.75	−0.85	−0.83	1.92
	6	9	682	1.81	1.00	0.66	−0.81	−0.82	1.63
C_6H_{13}	1	4	519	2.32	1.50	1.16	−0.82	−0.81	2.31
	2	5	582	2.13	1.31	0.97	−0.82	−0.80	2.11
	3	6	610	2.00	1.17	0.83	−0.83	−0.80	1.97
	4	7	642	1.93	1.08	0.74	−0.85	−0.81	1.89
	5	8	654	1.89	1.01	0.67	−0.83	−0.81	1.82
	6	9	680	1.82	0.99	0.65	−0.78	−0.81	1.80
$ROC_6H_4(CH{=}CH)_nPN$									
CH_3	4	9	499	2.48	0.085,0.69	0.07	−2.40	–	–
	6	11	528	2.35	0.081,0.65	0.04	−2.27	–	–
C_6H_{13}	4	9	498	2.49	0.084, 0.70	0.06	−2.41	–	–
	6	11	529	2.34	0.080, 0.66	0.03	−2.26	–	–
$ROC_6H_4(CH{=}CH)_nID$									
CH_3	4	7	576	2.15	0.44	0.12	−1.76	–	–
	6	9	618	2.01	0.36	0.03	−1.65	–	–
C_6H_{13}	4	7	576	2.16	0.45	0.12	−1.75	–	–
	6	9	616	2.01	0.37	0.04	−1.66	–	–

[a] λ_{onset} longest absorption wavelength at 10% of the UV peak maximum.
[b] $E_g^{opt} = 1240/\lambda_{onset}$.
[c] In CH_2Cl_2.
[d] In CH_3CN.
[e] $E_{red}^{calc} = |E_{ox}^1 - E_g^{opt}|$.
[f] $E_g^{CV} = |E_{ox}^1 - E_{red}^1|$.

the thermal stability slightly decreases with the increase in the length of the effective conjugation. This observation is in good agreement with some findings reported in the reference [23]. It should be noted, additionally, that the melting points of methoxy and hexyloxy derivatives with $n=6$ of both the PN and ID series are nearly identical. This observation can suggest that compounds with different alkyloxy groups in the benzene ring are thermally decomposed in a similar way, i.e., the first step of thermal decomposition leads to the same by product.

3.2. Experimental studies of solvent effects

The UV–vis spectra of all $ROC_6H_4(CH{=}CH)_nA$ were measured in non-polar (i.e., 2,2,4-trimethylopentane (TMP), CCl_4, tetrahydrofuran (THF), and CH_2Cl_2) as well as in polar (i.e., C_2H_5OH, CH_3OH, and CH_3CN) solvents at 25 °C. Typical absorption spectra for $C_6H_{13}OC_6H_4(CH{=}CH)_4TB$, $C_6H_{13}OC_6H_4(CH{=}CH)_4PN$, and $C_6H_{13}OC_6H_4(CH{=}CH)_4ID$ are shown in Fig. 3. The experimental values of π–π^* absorption bands (λ_{max}) and optical band gap (E_g^{opt}) for $ROC_6H_4(CH{=}CH)_4A$ are given in Tables 2 and 3.

As in other *all*-E polyenes described in the references [10,31–33] the optical spectra of the examined $ROC_6H_4(CH{=}CH)_nA$ (A = CP, ID, TB) are characterized by an intense, structureless and broad absorption band in the visible and ultraviolet region and the π–π^* transition is responsible for the first absorption band. Basing on data presented in Table 2, it can be concluded that elongation of the conjugated system results in a batochromic shift in UV–vis absorption spectra, revealed mainly by the fact that the addition of one conjugated bond induces a red shift as the length of the polyenic chain increases. Such a behavior confirms that the first absorption band is the π–π^* transition which position in the studied systems is practically independent on the alkyl chain length of the alkoxy substituent. At the same time there has been detected the hyperchromic shift for all studied polyenic structures. As in reference [32,33] the wavelength corresponding to the first absorption band maximum (λ_{max}) depends linearly upon the square root of the length of the complete π-electron conjugation n_{eff} (the effective length parameter, n_{eff} defines an equivalent contribution of the phenyl ring – it is two for each phenyl ring – to the conjugated electronic system). The obtained relationship is in accordance with the published data for ω-(*p*-alkoxyphenyl)polyenals [10] and *p*-substituted stilbene with alkoxy group [34]. Furthermore, the acceptor strength of D-π-A (A = PN, ID, TB) molecules (recalling data from Tables 2 and 3) decreases in the following order: TB > ID > CP. Additionally, for a fixed donor unit, the value of λ_{max} is the most red-shifted for the TB derivatives and it changes with the structure of A moiety in the same sequence. The absorption spectra presented in Fig. 3 demonstrate that in a strongly non-polar solvent as TMP the absorption bands of $ROC_6H_4(CH{=}CH)_nA$ with $n \geq 3$ show a weakly resolved vibronic structure and are significantly broadened in CCl_4. As expected, increasing polarity of the solvent causes a positive solvatochromism (e.g., for compound $C_6H_{13}OC_6H_4(CH{=}CH)_6TB$ ($n_{eff}=9$) in TMP, CCl_4, THF and CH_2Cl_2, $\lambda_{max}=593$, 586, 588, and 605 nm, respectively). Such a behavior was found to be characteristic also for other conjugated D-π-A systems, such as *p*-nitroaniline [35], terminally substituted stilbenes [36], biphenyls, and polyphenyls [37] and previously studied by us ω-(*p*-alkoxyphenyl)polyenals [10]. The observed changes of λ_{max}, with the increasing solvent polarity are about 9–13 nm and are comparable to those reported by Bourhill et al. [38] for

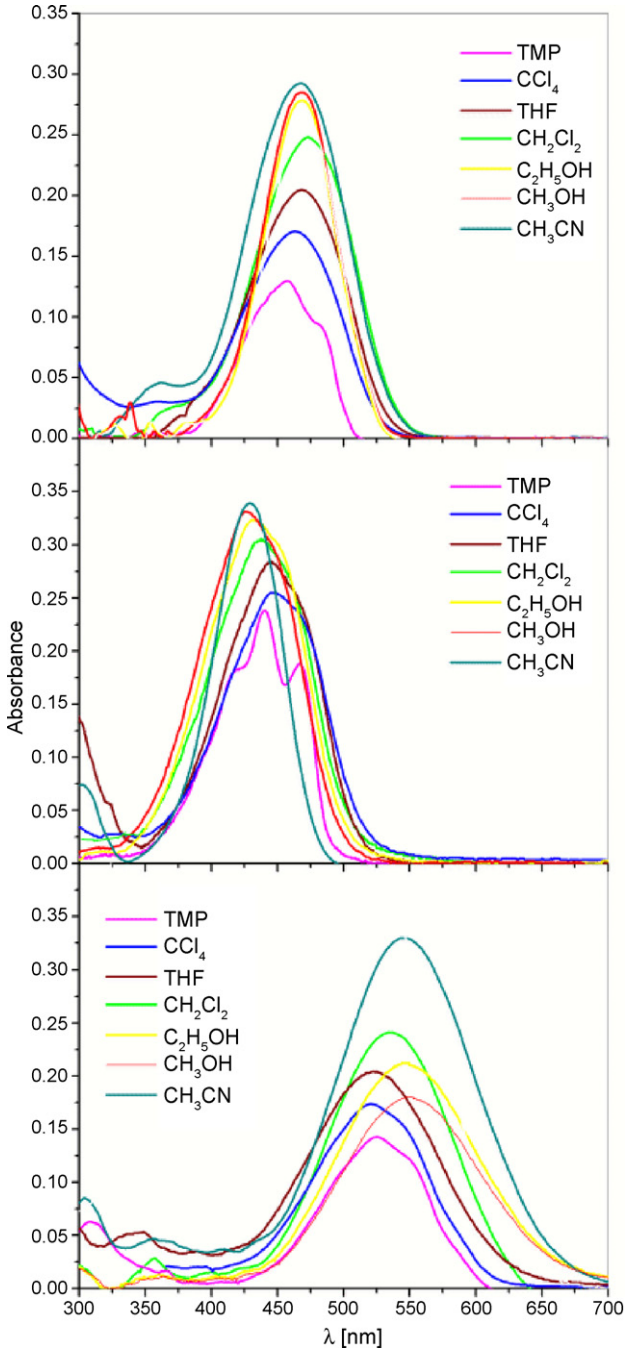

Fig. 3. UV–vis absorption spectra of polyenes (a) $C_6H_{13}OC_6H_4(CH{=}CH)_4ID$; (b) $C_6H_{13}OC_6H_4(CH{=}CH)_4PN$; (c) $C_6H_{13}OC_6H_4(CH{=}CH)_4TB$ in non-polar solvents (2,2,4-trimethylopentane (TMP), CCl_4, tetrahydrofuran (THF), CH_2Cl_2) and polar (C_2H_5OH, CH_3OH, acetonitrile (CH_3CN)) at 25 °C.

thiobarbituric acid derivatives containing three conjugated double bonds ($\Delta\lambda_{max} = 10$ nm). The shift of the absorption band towards the red indicates that with increasing solvent polarity, the energy of ground state is lowered less than that of the excited state. For all studied compounds in polar solvents (e.g., alcohols as C_2H_5OH, CH_3OH, and CH_3CN), a negative solvatochromism was observed which indicates that the polyenes dipole moment is being decreased due to the electronic transition. Thus, the studied polyenes, as thiobarbituric acid derivatives [38] and amphiphilic polyenals [10], show an inverted solvatochromism, i.e., their long wavelength solvatochromic absorption band exhibits first a batochromic and then a hypsochromic band shift, with the polarity of solvent. This is due to a solvent-induced change of the electronic ground-state structure from a less dipolar (in non-polar solvents) to a more dipolar (in polar solvents) chromophore with increasing solvent polarity. The decrease of the solute dipole moment during the electronic transition suggests [38,39] the shift of the electronic structure from a more polymethine-like state (with more strongly alternating π-electron density along the chain) to a more polyene-like state (with more balanced π-electron density) (see Fig. 4).

3.3. Electrochemical behavior

Since the electron transfer is central to the function of polyene bridge, an examination of the redox potentials of synthesized polyenes is pertinent. The electrochemical properties of $ROC_6H_4(CH{=}CH)_nA$ were studied by the cyclic voltammetry (CV) at the room temperature in CH_2Cl_2 or CH_3CN solutions, using Pt as the working electrode, SCE or Ag/AgCl as reference and $TBABF_4$ or $TBAPF_6$ as the supporting electrolyte. Measured oxidation (E_{ox}) and reduction (E_{red}) potentials as well as calculated optical (E_g^{opt}) and electrochemical (E_g^{cv}) band gaps are collected in Table 3. Additionally, there is shown Fig. 5 as an example for the CV curves recorded over the potential range of (−2.0 to +2.0 V) for $C_6H_{13}OC_6H_4(CH{=}CH)_4A$ (A = TB, Fig. 5a; A = ID, Fig. 5b; A = PN Fig. 5c).

As it comes from Fig. 5 and Table 3 the CV's of all studied compounds exhibit, independently on the alkyl chain, an irreversible one single electron or two single electron oxidation waves (attributed to both the *n*-alkoxy moiety, and conjugated spacer). It suggests according to reference [34] that all cation-radicals, and possibly also dication, formed in these systems are short life-time species. For all studied compounds the

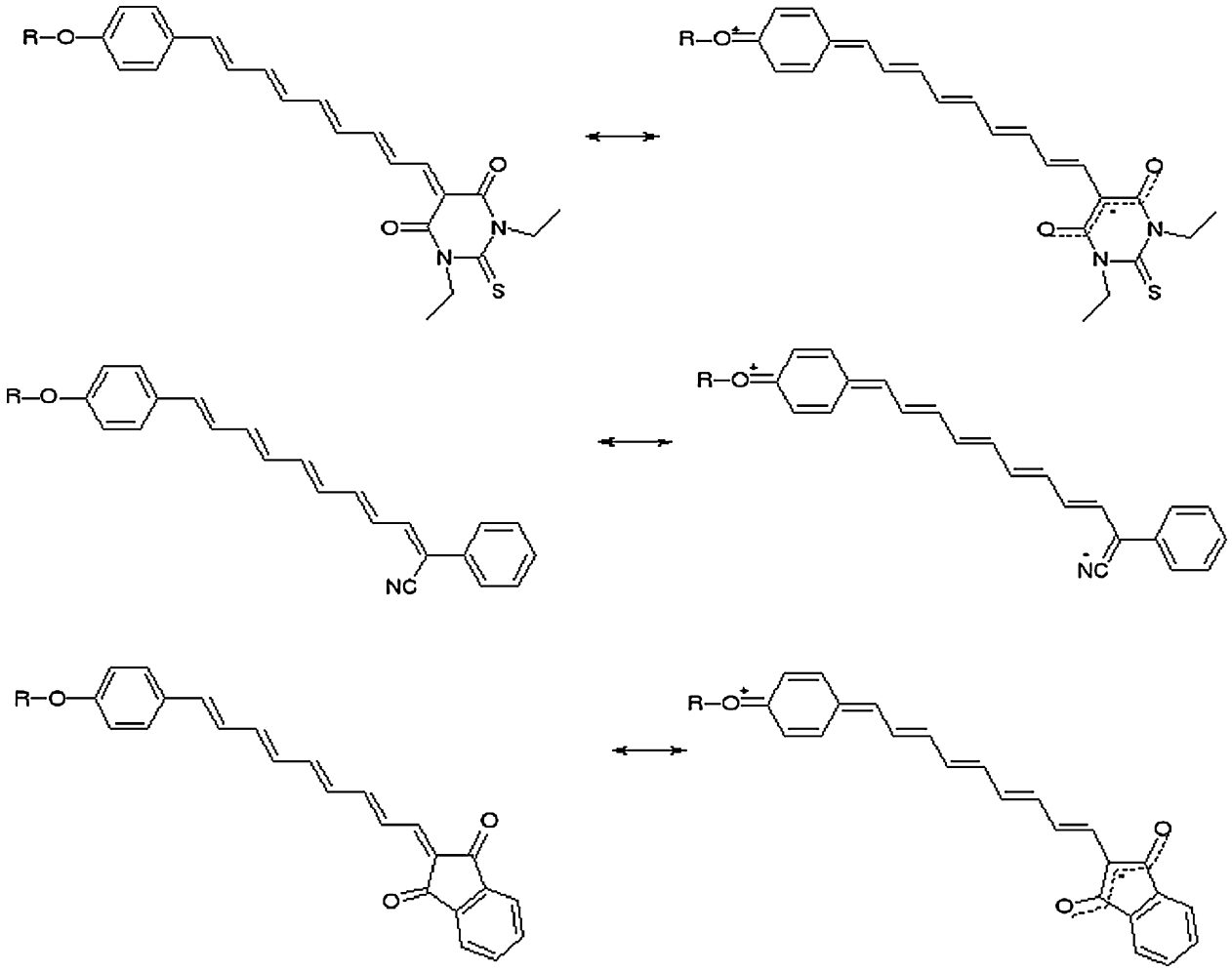

Fig. 4. Canonical charge -transfer resonance structures for a selected conjugated polyenes (a) $C_6H_{13}OC_6H_4(CH{=}CH)_4PN$, (b) $C_6H_{13}OC_6H_4(CH{=}CH)_4ID$, and (c) $C_6H_{13}OC_6H_4(CH{=}CH)_4TB$.

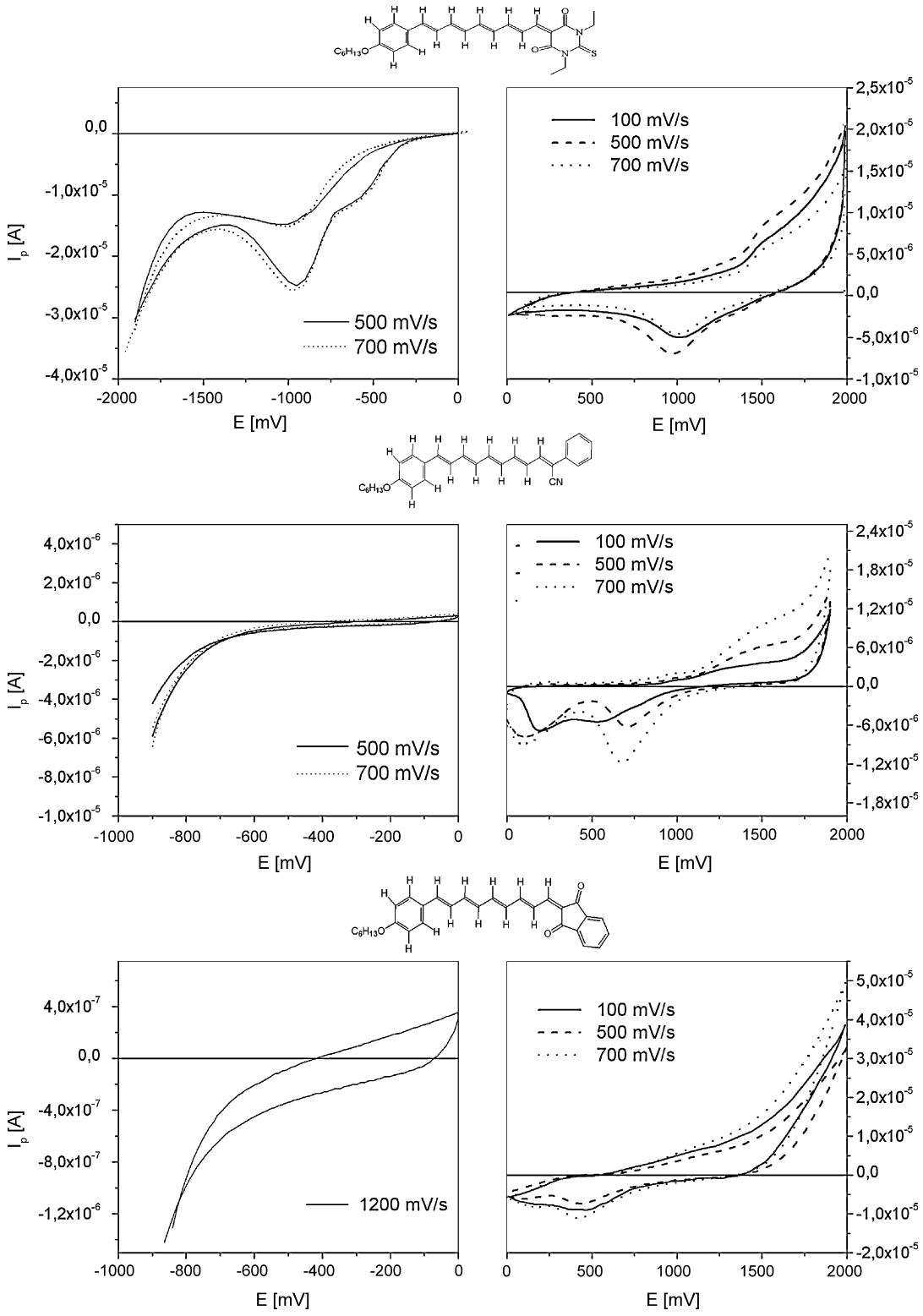

Fig. 5. Cyclic voltammograms of studied polyenes ($c = 1 \times 10^{-3}$ M) in 0.1 M $TBABF_4$ in CH_2Cl_2 (reduction), or 0.1 M $TBAPF_6$ in CH_2Cl_2 (oxidation).

exponential decrease in the oxidation potentials with the effective length of conjugated system is observed in CH_2Cl_2 and CH_3CN, which corresponds to the literature data for other *push-pull* conjugated structures [40]. The CV curves of $ROC_6H_4(CH{=}CH)_nPN$ ($n = 4$, 6) at a scan rate of 50 mV/s exhibit one very broad two-electron oxidation wave but when the scan rate increases up to ca. 100–700 mV/s a splitting of the wave into two components related to two one-electron processes has been occurring. This specific behavior of $ROC_6H_4(CH{=}CH)_nPN$ derivatives – similar to that observed for

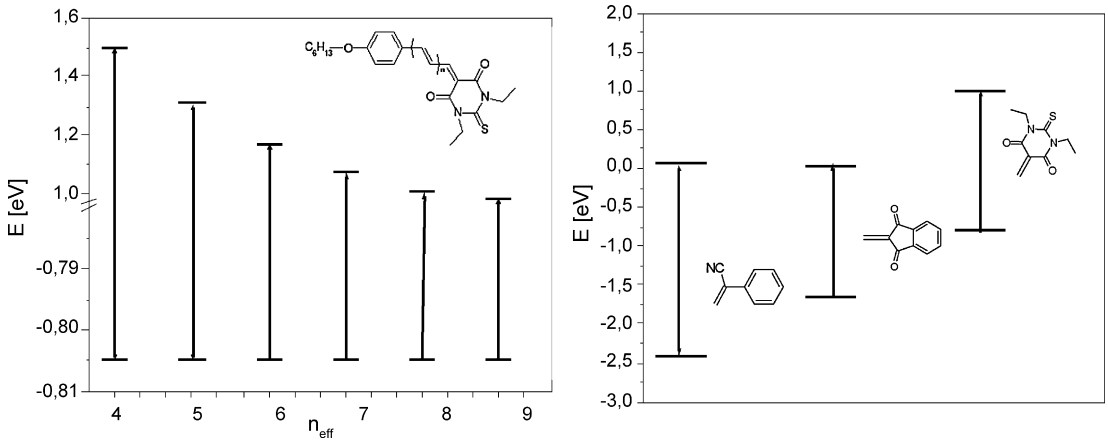

Fig. 6. Reduction and oxidation potentials (a) measured for $C_6H_{13}OC_6H_4(CH{=}CH)_4TB$ ($n_{eff} = n + 3$), (b) measured (oxidation) and calculated (reduction) for $C_6H_{13}OC_6H_4(CH{=}CH)_nA$, A = TB, PN, ID, $n_{eff} = 9$.

symmetrical carotenoids by Broszeit et al. [43] – makes possible to state that the influence of the alkoxy (donor) and phenylacetonitrile groups (acceptor) upon the polyenic bridge is not very strong. Such a conclusion was also confirmed by our NMR results (vicinal coupling constants of ca. 15 Hz, see Section 2—details related to the syntheses). For $ROC_6H_4(CH{=}CH)_nID$ and $ROC_6H_4(CH{=}CH)_nTB$ derivatives, however, there is no such a splitting under similar experimental conditions. The CV's of $ROC_6H_4(CH{=}CH)_nTB$ in the CH_2Cl_2 solution show irreversible reduction wave at scan rates up to 1000 mV/s. A peak potential at about −0,80 V is comparable to one earlier observed by Blanchard-Desce et al. [41] and Garin et al. [42] for thiobarbituric acid derivatives. The radical-anion wave is anodically shifted in compounds with A = TB, versus their carbonyl containing precursors due to the higher acceptor ability of the thiobarbituric chromophore.

From the CV and spectroscopic measurements one can calculate the energy gaps, E_g^{cv} and E_g^{opt}. The optical band gap, E_g^{opt} (Table 3) was calculated for studied polyenes $ROC_6H_4(CH{=}CH)_nA$ from the onset of the longest absorption wavelength at 10% of the UV peak maximum as indicated in [34]. It may be noted, that changes in the band gaps with structure match the red shift observed in the UV absorption spectra. For the CV measurements, E_{ox}^1, can be approximated as HOMO and E_{red}^1 as LUMO potentials [41–43]. The computed values of E_g^{opt} for thiobarbituric acid derivatives are close to those obtained from the CV technique E_g^{cv} (average standard deviation of 2.6%). Although, values of the band gap, E_g^{cv}, estimated as the difference between the first oxidation and reduction potentials are tightly correlated to those indicated by optical data, E_g^{opt}, though they are somewhat smaller. More electron rich molecule corresponds to the higher value of HOMO energy. The values of E_g^{cv} decrease with the increase in the value of n_{eff} (Fig. 6a) being in agreement with the tendency revealed by the UV–vis spectral data.

For the compounds $ROC_6H_4(CH{=}CH)_nPN$ as well as $ROC_6H_4(CH{=}CH)_nID$, we could calculate reduction potentials (E_{red}^{calc}) which are below −1.66 V. The expected value of the reduction potential for these polyenes is masked by the solvent break down so that we were not able to measure reduction potentials in our CV experiments. Fig. 6b shows the effect the structure of the electron acceptor moiety on the value of redox potentials and the band gap energy at constant value of $n_{eff} = 9$. For $ROC_6H_4(CH{=}CH)_nID$ and $ROC_6H_4(CH{=}CH)_nPN$ derivatives the HOMO energy was approximated by the experimental value of E_{ox}^1. Since the reduction potential could not be experimentally determined for these compounds, therefore, the LUMO energy was approximated by the value of E_{red}^{calc}. From the analysis of the same CV data we can also generally conclude that the increase of the acceptor strength corresponds to the increase in the absolute value of the HOMO and LUMO energy levels.

4. Conclusions

The reported, newly synthesized *push-pull* polyenes $ROC_6H_4(CH{=}CH)_nA$ ($n = 1$, 2, 3, 4, 5, and 6 for $R = C_6H_{13}$ and A = diethyl-thioxodihydropyrimidine-4,6-dione (TB) moiety; $n = 4$, 6 and for $R = CH_3$, C_6H_{13} and A = TB, 1,3-, indan-l,3-dione (ID) and phenylacetonitrile (PN) groupings) are stereo defined products (pure *all*-E configuration) which reveal a profound thermal stability, and well expressed spectroscopic and electrochemical behavior. Their decomposition temperature is the lowest for $ROC_6H_4(CH{=}CH)_nTB$ (133 °C ($n = 6$, $R = CH_3$) – 233 °C ($n = 1$, $R = C_6H_{13}$)) while highest for $ROC_6H_4(CH{=}CH)_nID$ derivatives (190 °C ($n = 4$, $R = CH_3$) – 291 °C ($n = 6$, $R = C_6H_{13}$)). They interact with solvent molecules in usual manner as described in the literature for other D-π-A derivatives and exhibit through bond intramolecular charge-transfer interactions. An increase in the polyenic linker length induces a batochromic shift of the absorption band, which levels off for the longest molecules studied and causes a narrowing of the band energy gap. A bathochromic shift of the value of λ_{max} occurs with the increase of D–A pair strength and an inverted solvatochromic effect is observed with the increase of the solvent polarity. The CVs of derivatives containing CH_3 and C_6H_{13} alkyl groups with the same A and n show almost the same irreversible oxidation waves in the measured potential range. Further work will be focused on the photoconductivity of described here compounds.

Acknowledgments

Supports of this work by the State Committee of Scientific Research (Grant No. 7 T09A 063 20) and the Faculty of Chemistry of Wroclaw University of Technology are gratefully acknowledged.

References

[1] J. Liu, R. Castro, K.A. Abboud, A.E. Kaifer, J. Org. Chem. 65 (2000) 6973–6977.
[2] R. Cammi, B. Mennucci, J. Tomasi, J. Am. Chem. Soc. 120 (1998) 8834–8847.
[3] M. Del Zoppo, A. Bianco, G. Zerbi, Synth. Met. 139 (2003) 881–884.
[4] S. Suresh, H. Zengin, B.K. Spraul, T. Sassa, T. Wadab, D.W. Smith Jr.a, Tetrahedron Lett. 46 (2005) 3913–3916.
[5] V.M. Geskin, C. Lambert, J.L. Bredas, J. Am. Chem. Soc. 125 (2003) 15651–15658.
[6] M. Dekhtyar, W. Rettig, Phys. Chem. Chem. Phys. 3 (2001) 1602–1610.
[7] B.W. Domagalska, L. Syper, K.A. Wilk, Synthesis 16 (2001) 2463–2469.
[8] B.W. Domagalska, L. Syper, K.A. Wilk, Tetrahedron 60 (2004) 1931–1939.
[9] B.W. Domagalska, K.A. Wilk, H. Szymusiak, R. Zielinski, Comput. Chem. 24 (2000) 359–367.
[10] B.W. Domagalska, K.A. Wilk, S. Wysocki, Phys. Chem. Chem. Phys. 5 (2003) 696–702.
[11] P.N. Prasad, D.J. Williams, Introduction to Nonlinear Optical Effect in Molecules and Polymers, Wiley, New York, 1990.
[12] M. Sczepan, W. Rettig, Y.L. Bricks, Y.L. Slominski, A.I. Tolmachev, J. Photochem. Photobiol. A, Chem. 124 (1999) 75–84.
[13] H. Braatz, S. Hecht, H. Seifert, S. Helm, J. Bendig, W. Rettig, J. Photochem. Photobiol. A: Chem. 123 (1999) 99–108.
[14] R. Lu, Y.S. Jiang, J.Q. Duo, X.D. Chai, W.S. Yang, N. Lu, Y.W. Cao, T.J. Li, Supramol. Sci. 5 (1998) 737.
[15] N. Di Cesare, J.R. Lakowicz, J. Photochem. Photobiol. A: Chem. 143 (2001) 39–47.
[16] G. Pistolis, A. Malliaris, Chem. Phys. 226 (1999) 83–99.
[17] P. Czerney, G. Graneß, E. Birckner, F. Vollmer, W. Rettig, J. Photochem. Photobiol. A: Chem 89 (1995) 31.
[18] W.L. Ryan, D.J. Gordon, D.H. Levy, J. Am. Chem. Soc. 124 (2002) 6194–6201.
[19] D. Beljonne, F. Meyers, J.L. Bredas, Synth. Met. 30 (1996) 211.
[20] G. Bartocci, G. Galiazzo, G. Gennari, E. Marri, U. Mazzucato, A. Spalletti, Chem. Phys. 272 (2001) 213–225.
[21] R. Alvarez, M. Herrero, S. Lopez, A.R. De Lera, Tetrahedron 54 (1998) 6793–6810.
[22] S.R. Marder, B. Kippelen, A. Yen, N. Peyghambarian, Nature 388 (1997) 845.
[23] B.W. Domagalska, K.A. Wilk, A. Chyla, L. Syper, in Surfactants and Dispersed Systems in Theory and Practice, KazimieraA. Wilk (Sci. Ed), Oficyna Wyd. PWr, 2003, pp. 271–276.
[24] T. Koźlecki, K.A. Wilk, R. Gancarz, J. Photochem. Photobiol. A: Chem. 116 (1998) 229–234.
[25] L. Zhivkov, G. Wang, S. Nespurek, B.W. Domagalska, K.A. Wilk, New Organic Materials for Sollar Cell Application, NATO Advanced Study Institute—Nanostructured and Advanced Materials for Optoelectronic, Photovoltaic and Sensor Applications, Sozopol, Bulgaria, 2004.
[26] A.J. De Lucas, N. Martin, L. Sanchez, C. Sesane, R. Andreu, J. Garin, J. Ordura, R. Alcala, B. Villacampa, Tetrahedron 54 (1998) 4655–4662.
[27] V. Alain, M. Blanchard-Desce, I. Ledoux-Rak, J. Zyss, Chem. Commun. (2000) 353–354.
[28] R.M. Silverstein, G.C. Bassler, T.C. Morrill, Spectrometric Identification of Organic Compounds, John Wiley & Sons, 1991.
[29] J. Wernly, J. Lauterwein, Helv. Chim. Acta 66 (1983) 1576.
[30] F. Steybe, F. Effenberger, S. Beckmann, P. Krämer, C. Glania, R. Wortmann, Chem. Phys. 219 (1997) 317.
[31] M. Blanchard-Desce, C. Runser, A. Fort, M. Barzoukas, J.M. Lehn, O. Bloy, V. Alain, Chem. Phys. 199 (1995) 253.
[32] A. Ulman, C.S. Willand, W. Köhler, D.R. Robello, D.J. Williams, L. Handley, J. Am. Chem. Soc. 112 (1990) 7083.
[33] D.L. Albert, J.O. Morley, D.J. Pugh, Chem. Phys. 99 (1993) 5197.
[34] H. Ndayikengurukie, S. Jacobs, W. Tachelet, J. Van Der Looy, A. Pollaris, H.J. Geise, M. Claeys, J.M. Kaufrman, S. Janitz, Tetrahedron 53 (1997) 13811.
[35] D. Gust, T.A. Moore, A.L. Moore, A. Barrett, L.O. Harding, L.R. Makings, P.A. Lidell, F.C. De Schryver, M. Van der Auweraer, R.F. Bensasson, M. Rougez, J. Am. Chem. Soc 110 (1988) 321.
[36] R.W.H. Berry, P. Brocklehurst, A. Burawoy, Tetrahedron 10 (1960) 109.
[37] D.W. Sherwood, M. Calvin, J. Am. Chem. Soc. 64 (1942) 1350.
[38] G. Bourhill, J.L. Bredas, L.T. Cheng, S. RMarder, F. Meyers, J.W. Perry, B.G. Tiemann, J. Am. Chem. Soc. 116 (1994) 2619.
[39] S.R. Marder, D.N. Beratan, L.T. Cheng, Science 252 (1991) 10.
[40] G. Märkl, A. Poll, N.G. Aschenbrenner, C. Schmaus, T. Troll, P. Kreitmeier, H. Noth, M. Schmidt, Helv. Chim. Acta 79 (1996) 1497.
[41] M. Blanchard-Desce, V. Alain, P.V. Bedworth, S.R. Marder, A. Fort, C. Runser, M. Barzoukas, S. Lebus, R. Wortmann, Chem. Eur. J. 3 (1997) 1091.
[42] J. Garin, J. Orduna, J.I. Rupérez, R. Alcalá, B. Villacampa, C. Sánchez, N. Martin, J.L. Segura, M. Gonzales, Tetrahedron Lett. 39 (1998) 3577–3580.
[43] G. Broszeit, F. Diepenbrock, O. Gräf, D. Hecht, J. Heinze, H.D. Martin, B. Mayer, K. Schaper, A. Smie, H.H. Strehblow, Liebiegs Ann./Recuel. (1997) 2205.